

---

# Analysis of statistical interpolation methods to generate the velocities model for continental Ecuador from GNSS data

---

**Análisis de métodos de interpolación estadística para generar el modelo de velocidades para el Ecuador continental a partir de datos GNSS**

**Análise de métodos de interpolação estatística para gerar o modelo de velocidade para o Equador continental a partir de dados GNSS**

---

**Marco P. Luna<sup>1</sup>, Alejandra Staller<sup>2</sup>, Alfonso Tierra<sup>1</sup>,  
Xavier Molina<sup>1</sup> & Theofilos Toulkeridis<sup>1,3</sup>**

<sup>1</sup> Universidad de las Fuerzas Armadas ESPE, Sangolquí, Ecuador

<sup>2</sup> Universidad Politécnica de Madrid, ETSI Topografía, Geodesia y Cartografía  
Campus Sur (UPM), Madrid, España

<sup>3</sup> Universidad de Especialidades Turísticas (UDET), Quito, Ecuador

[mpluna@espe.edu.ec](mailto:mpluna@espe.edu.ec); [a.staller@upm.es](mailto:a.staller@upm.es); [artierra@espe.edu.ec](mailto:artierra@espe.edu.ec);  
[pxmolina3@espe.edu.ec](mailto:pxmolina3@espe.edu.ec); [ttoulkeridis@espe.edu.ec](mailto:ttoulkeridis@espe.edu.ec)

Luna <https://orcid.org/0000-0003-1433-2658>

Staller <https://orcid.org/0000-0003-0335-0949>

Tierra <https://orcid.org/0000-0002-2885-0088>

Molina <https://orcid.org/0000-0001-8175-9331>

Toulkeridis <https://orcid.org/0000-0003-1903-7914>

---

### RESUMEN

Realizamos una comparación entre los métodos de interpolación de Kriging y Colocación de Mínimos Cuadrados. Así se obtuvo un modelo de velocidad óptimo de la corteza terrestre para el Ecuador continental a partir de un campo de velocidad ITRF2008 obtenido con datos GNSS en el período 2008-2014. El mejor ajuste para los dos componentes fueron el semivariograma esférico y estable. El modelo funcional para el método de colocación de mínimos cuadrados fue de tercer orden para el componente Este y de segundo orden para el componente Norte. Los resultados obtenidos se compararon con la velocidad de las estaciones GNSS utilizadas para la verificación y utilizando la técnica de validación cruzada. Todas las estadísticas favorecen el método de Colocación de Mínimos Cuadrados, ya que presenta un mejor ajuste y confiabilidad para representar el modelo de velocidad del Ecuador continental.

**PALABRAS CLAVE:** Kriging; colocación de mínimos cuadrados; validación cruzada; semivariogramas; modelo de velocidades.

### RESUMO

Realizou-se uma comparação entre os métodos de interpolação de Kriging e Colocação de Mínimos Quadrados. Isso permitiu obter um modelo de velocidade ótima da crosta terrestre para o Ecuador continental a partir de um campo de velocidade ITRF2008 obtido com dados GNSS no período 2008-2014. Os semivariogramas com melhor ajuste para os dois componentes foram o semivariograma esférico e estável. O modelo funcional para o método de Colocação dos Mínimos Quadrados foi de terceira ordem para a componente Leste e de segunda ordem para a componente Norte. Os resultados foram comparados com a velocidade das estações GNSS utilizadas para verificação e empregando a técnica de validação cruzada. Todas as estatísticas favorecem o método de Colocação dos Mínimos Quadrados, toda vez que apresenta um melhor ajuste e confiabilidade para representar o modelo de velocidade do Ecuador continental.

**PALAVRAS-CHAVE:** Kriging; Colocação de Mínimos Quadrados; validação cruzada; semivariogramas; modelo de velocidades.

### ABSTRACT

We performed a comparison between the interpolation methods of Kriging and Least Squares Collocation. This allowed to obtain an optimal velocity model of the earth's crust for continental Ecuador from a velocity field ITRF2008 obtained with GNSS data in the period 2008-2014. The best fitting semivariograms for the two components were the Spherical and Stable semivariogram. The functional model for Least Squares Collocation method was of third order for the East component and of second order for the North component. The results obtained were compared with the velocity of the GNSS stations used for verification and using the cross-validation technique. All the statistics favor the least squares Collocation method since it presents a better fit and reliability to represent the velocity model of continental Ecuador.

**KEYWORDS:** Kriging; least-squares collocation; cross-validation; semivariograms; velocities model.

## 1. Introduction

Global Navigation Satellite Systems (GNSS) use geocentric reference system to position any point (Dow *et al.*, 2009; Pascual-Sánchez, 2007; Rajner & Liwosz, 2017). This causes the coordinates of the point located on the earth's surface and positioned at a certain epoch to change over time due to the movement of tectonic plates (Mather *et al.*, 1979; Perez *et al.*, 2003; Banko *et al.*, 2020). Due to this movement, it is necessary to make corrections in the corresponding coordinates, and for this the movement speed of the point must be calculated (Denker *et al.*, 2018; Gili *et al.*, 2000; Yang & Qin, 2021). There are velocity models used worldwide but for the American continent, Drewes & Heidbach (2005) presented the first crustal velocity model for South America, named VEMOS (Velocity Model of South America), which was obtained from geodetic observations conducted throughout the region (Sánchez *et al.*, 2018; Da Silva *et al.*, 2018; Montecino *et al.*, 2017).

Currently, Sánchez & Drewes (2020) present the VEMOS 2017 velocity model, using the Least Squares Placement method, while Cisneros & Nocquet (2011) obtained the first velocity field for Ecuador. From this velocity field, Tierra (2016) presented the first model of velocities of the Earth's crust at a national level using the artificial neural networks method through supervised learning. Later Luna *et al.* (2017) presented a velocity model for Ecuador using the Universal Kriging method.

The velocity model to be obtained in this study must consider their spatial variations, therefore a totally deterministic solution to our problem would not be the most convenient (Webster & Oliver, 2007). Probabilistic methods, in addition to considering spatial proximity, also consider the existence of spatial autocorrelations between the sampled points, and from this they deduce that these autocorrelations must be valid for the values of the points to be estimated (Yan *et al.*, 2021; Xie *et al.*, 2017; Wilde *et al.*, 2018).

Given that the factors that affect the values of the velocities are numerous, largely unknown in detail and interact with a complexity that we cannot unravel, it can be said that the results are affected by random errors. Since our objectives are predominantly to describe quantitatively how the velocities vary spatially, as well as to estimate or predict their values in unsampled sites and to estimate the prediction errors in order to be able to judge what confidence to place in them, models with a probabilistic and stochastic approach have been considered as best suited for our purpose. Considering that, two interpolation

methods were selected, being the Kriging Estimation Method and the Least Squares Collocation Method (LSC). These methods will be used to make a comparison and suggest the most suitable for this study (Jiang *et al.*, 2020; Ling *et al.*, 2019; Yang & Cheng, 2020; Xiao *et al.*, 2020; Fu *et al.*, 2020; Zeng *et al.*, 2019; Shapeev *et al.*, 2019).

In order to calculate the velocity model for continental Ecuador, the velocity field obtained from the processing and analysis of the time series of 33 continuous monitoring stations of the REGME network (Red GNSS de Monitoreo Continuo del Ecuador) is available (Luna *et al.*, 2017). In addition, to having greater data coverage, 131 speeds of the passive stations of the RENAGE network (National GPS Network of Ecuador) were used, obtained from the portal of the Military Geographical Institute of Ecuador (Cisneros & Nocquet, 2011).

## 2. Methodology

For the Kriging estimation, the Universal Kriging technique was used because the speeds of the stations indicate a trend in the eastern and northern components (Michael *et al.*, 2019; Shukla *et al.*, 2020; Lin *et al.*, 2018). Spherical and stable semivariograms were used for the structural analysis (Obroślak & Dorozhynskyy, 2017; Verma *et al.*, 2018; Kesuma *et al.*, 2019). The functional models selected for LSC prediction were chosen considering the best fit and also that they are well conditioned (Erol & Erol, 2021). The bad conditioning of a system is induced by small variations in the values of the matrices that intervene in the adjustment, these variations would cause a small determinant and a large inverse matrix that would influence the inference of the results (Sevilla, 1987). For the verification, a set of 16 stations that did not enter into the determination of the model were selected and compared by cross-validation, which consists of excluding the observation of one of the  $n$  sample points, and with the remaining  $n-1$  values predicting the value of the variable at the place of the point that was excluded. We make a brief explanation of the methods to use.

### 2.1 Kriging

Estimation is the task for which geostatistics was initially developed and is called Kriging, in honor of D. G. Krige (1951). It was further developed by Matheron (1971), e.g., Blais (1982), Journel and Huijbregts (1991), Reguzzoni *et al.* (2005). The Kriging estimator is a linear estimator given that the predicted value is obtained as a linear combination of known values (Matheron, 1971), it is also based on the principle of least squares, which is why some

authors (Cressie, 1993) also define it as optimal predictor or best linear predictor. Different types of Kriging are applied depending on the properties of the stochastic process or the random field. The Kriging method, which is based on the theory of regionalized variables (Journel & Huijbregts, 1978; Goovaerts, 1997), is increasingly used because it allows capitalizing the spatial correlation between neighboring observations to predict attribute values at unsampled locations (Oreajuela *et al.*, 2021).

### 2.1.1 Exploratory data analysis

Once the continuous monitoring stations have been selected for modeling, the exploratory data analysis is performed using descriptive statistics such as: mean, standard error, median, standard deviation, variance, coefficient of skewness and box plots. The variability of the data allows, at a first glance, to determine which ones will have a lower prediction error (Webster & Oliver, 2007). This analysis is important in order to determine outliers and establish whether some assumptions of geostatistical theory are valid or to define which prediction procedure is the most convenient to use.

The identification of atypical velocity values is considered important within geostatistical analysis given that there are certain models used that are very sensitive to these values (Webster & Oliver, 2007; Lobo & Fonseca, 2020), therefore, special care needs to be taken in predictions performed near these points. Hereby, a fundamental graph is the scatter plot both for detecting relationships between variables and for identifying trends, since this would be one of the conditions that would determine the Kriging method to be used (FIGURE 1).

The scatter plots with respect to the longitude and latitude coordinates allows to appreciate a trend of the velocity in the East and North components along these directions. This dispersion determines that its average value is not constant throughout the region, therefore the most appropriate technique is Universal Kriging since it recognizes the non-stationary deterministic and random components in a variable. This technique estimates the trend in the former and the latter's variogram and recombines the two for prediction.

### 2.1.2 Structural analysis

Since geostatistics treats a set of spatial data as a sample from performing a random process, the analysis needs to include spatial correlation. If the phenomenon fulfills the stationarity assumption, any of the three spatial correlation functions may be used, being variogram or semi-variogram, covariogram, and correlogram. However, in practice the semivariogram is more often used as it is not necessary to perform an estimation of parameters as in the case of the other functions (Webster & Oliver, 2007). The semivariogram is expressed with the following equation:

$$\gamma(h) = \frac{\sum(Z(x+h) - Z(x))^2}{2n} \quad (1)$$

Where  $Z(x)$  is the value of the variable at position  $x$ ,  $Z(x+h)$  is another sample value separated from the previous one by a distance  $h$ , and  $n$  is the number of pairs that are separated by the given distance (Webster & Oliver, 2007).

The experimental semivariogram is obtained through the calculation of the semivariance functions for various values of  $h$ . Due to the irregularity of the sampling and the distance of the sampled sites, intervals of  $\{(0, h], (h, 2h], (2h, 3h], \dots\}$  are determined to obtain the experimental semivariogram. From this semivariogram we obtain the average of the distances for each interval with its corresponding semivariance value. Defining the value of  $h$  is able to affect the resulting semivariogram, therefore this value should be chosen carefully. If the  $h$  value is low, then there may be few comparisons in each interval, leading to an experimental semivariogram that appears erratic. If, on the other hand, the  $h$  value is high, then it is likely that there are few estimate values and the detail is lost.

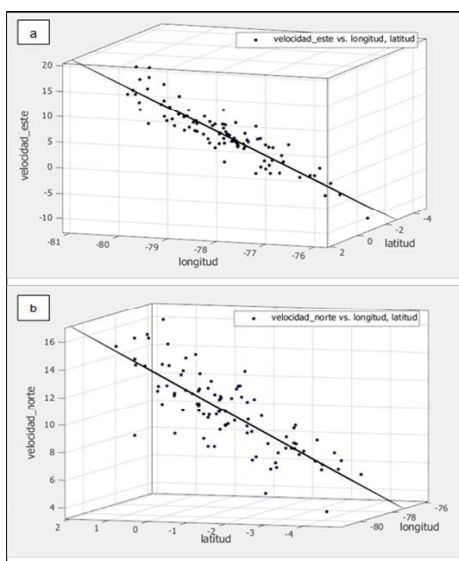


FIGURE 1. Scatter plot of velocity values with respect to geographic coordinates. a) East component, b) North component

Given that our data are present in a spatially irregular distribution, we used the criterion of Johnston *et al.* (2001) where it has been indicated an average distance  $h$  determined by the equation:

$$h = \sqrt{\frac{A}{n}} \quad (2)$$

Where  $A$  is the research area and  $n$  is the number of measured points.

The distance  $h$  can also be determined empirically as the minimum mean distance between observed points.

$$h = \frac{1}{n} \sum_{i=1}^n \min(D|ij), j = 1, n, j \neq i \quad (3)$$

Where  $n$  is the number of measured points.

As will be explained and indicated later, in order to solve the prediction problem, it is necessary to know the correlation structure of the data for any distance between the different points within the study area. The experimental semivariogram has only been obtained for some averages of distances, so if we require its value for any distance, it is necessary to have a theoretical model of semivariance that fits the experimental semivariogram as closely as possible, which is obtained with the sample data. All semivariogram models have three common parameters which are nugget ( $C_0$ ), sill ( $C_1$ ), and range ( $a$ ), as illustrated in **FIGURE 2**.

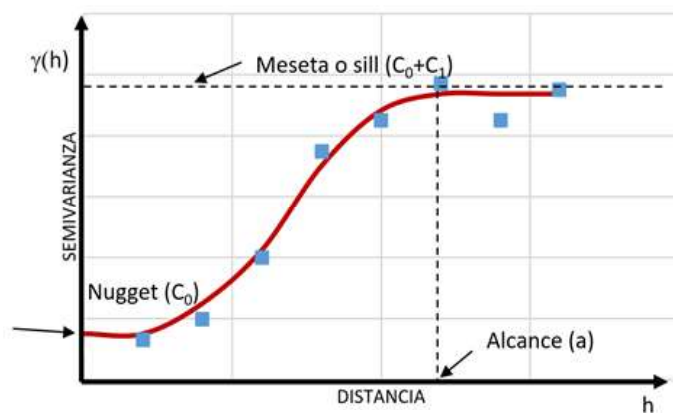


**FIGURE 2.** Parameters of a theoretical semivariogram model [5]. The solid red line represents the theoretical semivariogram, while the blue dots represent the experimental semivariogram

The nugget effect is the punctual discontinuity at the origin and is produced by measurement errors in the variable or at its scale. This value should not exceed 50% of the sill value. The sill represents the upper bound of the semivariogram and the range represents the distance from which two observations are independent. For geostatistical approaches to be effective, the spatial correla-

tion range for a given variable (defined by the variogram) needs to be greater than the average distance between the sample points. Otherwise, Kriging will only provide a robust estimate in the local neighborhood of each of the data points in the training sample (Scull *et al.*, 2005). The experimental semivariogram has only been obtained for some distances averages, therefore it is necessary to have a theoretical semivariogram model that best fits, considering for this purpose the models recommended by Webster & Oliver (2007). These semivariogram models are theoretically well founded, which needs to be adapted to the experimental values and select the most appropriate model.

### 2.1.3 Prediction

Universal Kriging proposes that the value of the variable can be predicted as a linear combination of the  $n$  random variables like this:

$$Z(x_0) = \sum \lambda_i Z(x_i) \quad (4)$$

Where  $Z(x_i)$  are the measured values and  $\lambda_i$  are the weights of the original values.

When the data are characterized by presenting a trend, it is common to decompose the variable  $Z(x)$  as the sum of the trend, treated as a deterministic function, plus a stationary random component with zero mean. That means:

$$Z(x) = m(x) + \varepsilon(x) \quad (5)$$

With  $E(\varepsilon(x))=0$ ,  $V(\varepsilon(x))=\sigma^2$  therefore  $E(Z(x))=m(x)$ . The trend may be expressed by:

$$m(x) = \sum_{i=1}^p a_i f_i(x) \quad (6)$$

Where the deterministic functions  $f_i(x)$  are known and  $p$  is the number of terms used to fit  $m(x)$ .

In order to obtain the weights, the variance of the prediction error must be minimized with the condition of unbiased (sum of weights equal to 1) resulting in a system of equations that in the matrix form results:

$$\begin{pmatrix} \gamma_{11} & \dots & \gamma_{1n} & f_{11} & \dots & f_{p1} \\ \vdots & \ddots & \vdots & \vdots & \ddots & \vdots \\ \gamma_{n1} & \dots & \gamma_{nn} & f_{1n} & \dots & f_{pn} \\ f_{11} & \dots & f_{1n} & 0 & \dots & 0 \\ \vdots & \ddots & \vdots & \vdots & \ddots & \vdots \\ f_{p1} & \dots & f_{pn} & 0 & \dots & 0 \end{pmatrix} \cdot \begin{pmatrix} \lambda_1 \\ \vdots \\ \lambda_n \\ \mu_1 \\ \vdots \\ \mu_p \end{pmatrix} = \begin{pmatrix} \gamma_{10} \\ \vdots \\ \gamma_{n0} \\ f_{10} \\ \vdots \\ f_{p0} \end{pmatrix} \quad (7)$$

The prediction variance of Universal Kriging is expressed by [15]:

$$\sigma_{ku}^2 = \sum_{i=1}^n \lambda_i \gamma_{i0} + \sum_{k=1}^p \mu_k f_k x_0 \quad (8)$$

## 2.2 Least Squares Collocation (LSC)

The LSC is an interpolation method derived from geodesic sciences, which has been first introduced by H. Moritz (1978), in order to determine the shape of the earth and the gravitational field. The LSC method can be interpreted as a statistical estimation method that combines least squares fit and least squares prediction. LSC is widely used in Geodesy and related fields as demonstrated by various classical studies (Krarup, 1969; Moritz, 1978; Tscherning, 1976; Rummel, 1976; Kearsley, 1977; Moritz, 1980; Dermanis, 1980; Knudsen, 1987; Forsberg, 1987; Schaffrin, 1989). It constitutes a very general case of least squares. This technique combines adjustment, filtering, and prediction (FIGURE 3), and in this sense generalizes the adjustment problem (Sevilla, 1987).

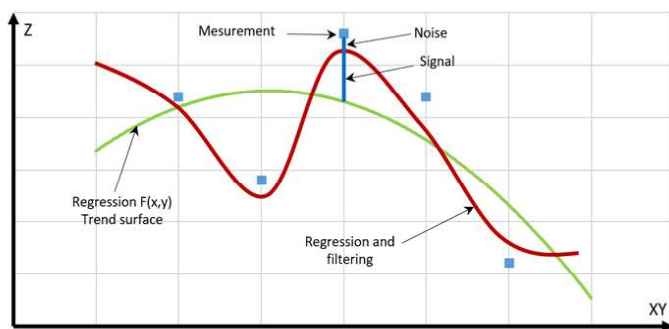


**FIGURE 3.** Pleast Squares Collocation Model (LSC). The blue points correspond to the measured values. This measure is composed of signal and noise. The green line is the functional model obtained by linear regression and the red line is the function determined by regression once the measurements have been filtered

### 2.2.1 Functional model

In the functional model with LSC, in addition to the parameters and the observation errors, the random part of mathematical expectation equal to zero is included, which

are the noise and the signal. The model is expressed as:

$$AX + L = V \quad (9)$$

Where  $X$  is the vector of the corrections of the model parameters,  $A$  is the design or coefficient matrix of the model,  $f_i(x)$  is the vector of the approximate observations and  $V$  are the observation errors.  $V$  is defined as follows:

$$V = s + r \quad (10)$$

Where  $r$  is the random measurement error which is defined as noise, and  $s$  is called signal and is the other random part of the field where the experiment is carried out, independent of the measurement method and equipment (Moritz, 1980).

The solution is obtained by the method of least squares using the equation:

$$X = (A^T P A)^{-1} (A^T P L) \quad (11)$$

Where  $P$  are the weights of the observations.

### 2.2.2 Stochastic model

The stochastic model is used in the fit in order to introduce information about the quality of the observations and the possible correlation between them (Leick, 1995). This is done using the variance-covariance matrix of the observations.

The variance - covariance matrix is given by:

$$\hat{C} = V \cdot V^T \quad (12)$$

The covariance matrix of the observations can be decomposed into covariances of the signals and noises:

$$\hat{C} = C_{SS} + C_{SS} \quad (13)$$

This covariance matrix corresponds only to values in the sampled sites; therefore, a covariance function must be determined for any point within the study area, called empirical covariance. For this reason, a specific polyno-

mial type function is obtained using least squares (FIGURE 4). The correlation length is similar to the range in the Kriging method (Odera *et al.*, 2012).

The resulting function is used to determine the  $C_{zz}$  matrix of the points at which the prediction is to be made, this means, calculate  $C(dz)$ .

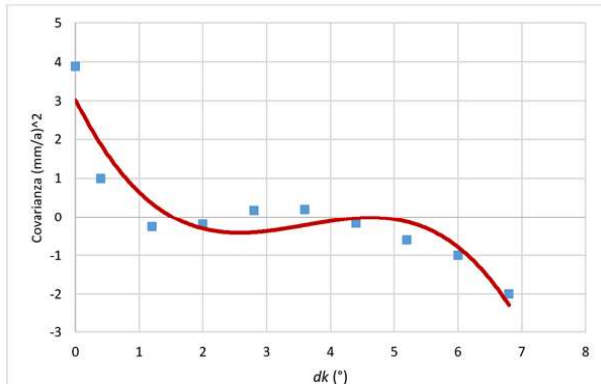


**FIGURE 4.** Empirical covariance. The blue points correspond to the average of the covariance values within each interval and the red line correspond to the functional model of the empirical covariance

Finally, the covariance matrix of the observations is expressed as:

$$\hat{C} = C_{SS} + C_{rr} = C(d) + \sigma_0^2 I \quad (14)$$

In matrix form is written as:

$$\hat{C}(d_{ij}) = \begin{bmatrix} C(0) & \dots & C(d_{1n}) \\ C(d_{12}) & \dots & C(d_{2n}) \\ \vdots & \ddots & \vdots \\ C(d_{n1}) & \dots & C(0) \end{bmatrix} + \begin{bmatrix} \sigma_0^2 & \dots & 0 \\ 0 & \dots & 0 \\ \vdots & \ddots & \vdots \\ 0 & \dots & \sigma_0^2 \end{bmatrix} \quad (15)$$

### 2.2.3 Prediction

In this case, the solution of the parameters is similar to the one calculated with least squares given in equation (11), where instead of using the weight matrix the empirical covariance matrix is used.

$$X_{LSC} = (A^T \hat{C}^{-1} A)^{-1} (A^T \hat{C}^{-1} L_{LSC}) \quad (16)$$

The signals for the observations are calculated with:

$$s = C_{SS} \hat{C}^{-1} V \quad (17)$$

Similarly, the signals can be estimated for any other unobserved point:

$$z = C_{zs} \hat{C}^{-1} V \quad (18)$$

With these signals, the filtering is performed at the original  $n$  observation points by applying the following equation:

$$L_s = L_0 + AX - s \quad (19)$$

In the new observations  $L_s$ , the observation errors no longer appear because the filtering has been performed, and it allows to calculate a new vector that we will call  $L_{LSC}$ . For the prediction at the unsampled points, the values of the  $z$  signal, determined in equation (18), are used, the values of the parameters adjusted by means of XLSC least squared placement, obtained in equation (16).

$$L_z = L_{0z} + B \cdot X_{LSC} - z \quad (20)$$

Where  $B$  is the design or coefficient matrix of the model corresponding to the points to be predicted and  $L_{0z}$  is the vector of approximate observations of these given points.

The prediction variance of is given by Ligas & Kullczycki (2010):

$$\sigma_k^2 = C(0) - c^T \cdot C^{-1} \cdot c \quad (21)$$

Where  $C(0)$  is the covariance when the distance  $d=0$ , that is, at the same point,  $C$  is the covariance matrix between the observed values and  $c$  is the vector of covariances between the observed and unobserved values.

### 3. Results and discussion

Before obtaining velocities, it is necessary to determine the value of  $h$  (lag), which will serve to determine the experimental semivariogram and the empirical covariance in the two methods studied. The values  $0.4^\circ$  and  $0.3^\circ$  obtained from (2) and (3) respectively were used. These values serve as a starting point to obtain  $h$  where the number of pairs is more representative for all intervals. That is, there are no intervals where the number of pairs is too small and others with very high values. As selection criterion for  $h$ , those in which the number of pairs has less dispersion were chosen. Table 1 lists the values of the dispersion of the number of pairs for each value of  $h$ .

**TABLE 1.** Variability of the number of pairs for each value of h

$h(^{\circ})$	$\sigma(^{\circ})$
0.29	375.38
0.30	339.76
0.31	302.29
0.32	279.70
0.33	279.69
0.34	279.68
0.35	279.67
0.36	267.71
<b>0.37</b>	<b>263.53</b>
0.38	272.35
0.39	283.38
0.40	292.37
0.41	302.97
0.42	319.98

**TABLE 1** indicates that for a value of  $h = 0.37$  there is greater uniformity in the number of pairs for each interval. With the velocities in the two components ( $V_e$  and  $V_n$ ) of the different stations, the purpose is to describe quantitatively how the velocities vary spatially and to estimate their values in unsampled sites using models that better fit the behavior of the movement of the Earth's crust in the study area. For this, the root mean square error ( $rms$ ) and the prediction variance are considered for comparison. The results of the proposed techniques are analyzed below.

### 3.1 Kriging

For the selection of the theoretical semivariogram, among the different types of models, those whose squared deviations with respect to the experimental semivariogram were the lowest were chosen. The spherical and stable semivariograms were chosen with the least variation, as listed in **TABLE 2**.

With these semivariograms, the prediction is performed and subsequently the verification with the 16 selected points. The results are listed in **TABLE 3**.

According to the calculated  $rms$  values, it is evident that the lowest value corresponds to the spherical model for both components in the prediction of the verification points. In **TABLE 4** we present the statistics obtained by applying cross-validation to the spherical and stable semivariogram models.

**TABLE 2.** Values of the parameters of the theoretical semivariograms with their respective mean square error

Model	$V_e (mm/a)$					$V_n (mm/a)$				
	$C_0$	$C_1$	$a$	$\Theta$	$rms$	$C_0$	$C_1$	$a$	$\Theta$	$rms$
Circular	0.00	41.60	4.65		2.77	0.00	10.80	4.65		0.77
Stable	1.16	48.00	4.02	1.89	0.86	1.78	12.00	5.00	1.89	0.36
ESpherical	0.00	48.2	5.03		1.43	0.00	13.02	5.44		0.40
Penta Spherical	0.00	42.35	4.65		1.98	0.00	10.80	4.65		0.62
Exponential	0.00	42.80	4.65		2.78	0.00	11.20	4.65		0.70

**TABLE 3.** Mean square error of the verification points using the spherical and stable semivariogram models in its two components

Model	$V_e (mm/a)$	$V_n (mm/a)$
	$rms$	$rms$
Spherical	1.37	0.88
Stable	1.54	0.98

**TABLE 4.** Statistical values for the spherical and stable models in their two components through cross validation

Model	$V_e (mm/a)$		$V_n (mm/a)$	
	$rms$	$\sigma^2$ of Prediction	$rms$	$\sigma^2$ of Prediction
	Spherical	1.76	5.19	1.81
Stable	2.01	1.82	2.44	1.78

The  $rms$  values favor the spherical model for both components, however, it can be seen that the prediction variance in the Eastern component for the spherical model is very high, this is due to the fact that the fit to the experimental semivariogram was less than the stable semivariogram.

### 3.2 LSC

The selected functional models were considered taking into account the best fit and that they are well conditioned. **TABLE 5** presents the mean square error values for the two components obtained from the verification data.

**TABLE 5.** Mean square error of validation for LSC

Technique	$V_e$ (mm/a)		$V_n$ (mm/a)	
	rms		rms	
LSC	1.22		0.95	

Next, **TABLE 6** presents the statistics obtained from applying the cross-validation using LSC for the two components.

**TABLE 6.** Statistical values for the LSC model in its two components from cross validation

Technique	$V_e$ (mm/a)		$V_n$ (mm/a)	
	rms	$\sigma^2$ of the prediction	rms	$\sigma^2$ of the prediction
LSC	1.70	2.30	1.73	1.39

The values indicate a great approximation in all the estimated points, which shows that the selection of the functional models and the covariance function were the most appropriate.

### 3.3 Comparison

**TABLE 7** lists the information of the statistics obtained for each prediction technique. It is observed that in Kriging method, the theoretical semivariograms that best fit the experimental semivariograms have a lower prediction variance, but not a better estimate.

For the East component, the models obtained with spherical Kriging and LSC have better values in the prediction of the points with rms = 1.76 mm / year and rms = 1.70 mm/year respectively, compared to the stable model with rms = 2.01mm / year. However, its precision is better because it has a lower value in the prediction variance. For the North component, the models obtained with spherical Kriging and LSC have better prediction values with rms = 1.81 mm/year and rms = 1.73 mm / year respectively, compared to the model obtained with stable Kriging that has rms = 2.44 mm / year. In this component, the models obtained with spherical Kriging and LSC have better accuracies with respect to the model obtained with stable Kriging.

**TABLE 8** indicates the results of the three prediction techniques by verification using 16 speeds that were not considered in the models.

**TABLE 7.** Statistical values for the different techniques used in cross-validation verification

Techniques	$V_e$ (mm/y)		$V_n$ (mm/y)	
	rms	$\sigma^2$ of Prediction	rms	$\sigma^2$ of Prediction
Spherical Kriging	1.76	5.18	1.81	1.24
Stable Kriging	2.01	1.50	2.44	1.63
LSC	1.70	2.30	1.73	1.39

**TABLE 8.** Mean square errors obtained from the verification data in the different spatial prediction models

Techniques	$V_e$ (mm/y)	$V_n$ (mm/y)
	rms	rms
LSC	1.22	0.95
Spherical Kriging	1.37	0.88
Stable Kriging	1.54	0.98

For the East component, the method that best performs the prediction is the LSC method, while for the North component the best prediction corresponds to spherical Kriging, considering that the stations that served for verification were randomly selected. Therefore, the method that best performs the prediction is the LSC, with small differences with Kriging with spherical semivariogram. These small differences are due to the fact that both methods follow the principle of minimizing the variance of the prediction error when the underlying function is considered as a second-order stochastic process with a known or estimated covariance function (Dermanis, 1984). Odera *et al* (2012) consider that although LSC may be the preferred technique for combining data, including parameter estimation, Kriging is relatively less laborious, faster, and works quite well. Although the data in this study cover a maximum distance of approximately 700 km, Darbeheshti & Featherstone (2009) consider that the LSC technique has been better applied at local and global scales, while Kriging is implemented at local scales, for distances no greater of 100 km.

Summarizing, we may note some advantages of the LSC method, such as it makes a better prediction according to the comparison made with the values for verifica-

tion and through cross-validation, the distribution of the data does not have to respond to established patterns, it offers the possibility of filtering observations, it is a best unbiased linear estimator, it minimizes the variance of the prediction error, and, it is best applied at local and global scales. However, simultaneously, there are also some disadvantages involved when using the LSC method, as that special care needs to be taken not to choose badly conditioned functions or matrices. Furthermore, one of the trickier parts is determining the empirical covariance function, and the determined covariance function will worse represent the edges of the area from which the data originated.

The same counts by the use of the Krigin method, where the advantages lie on hand as the Semivariograms summarize the spatial relationships of the data, the sum of the weights obtained is equal to 1, so that the expectation of the predictor is equal to the expectation of the variable, it is the best unbiased linear estimator, it mini-

mize the variance of the prediction error, and, when the primary variable observations are sparsely sampled, they can be supplemented with secondary variables that are sampled more densely, using cokriging.

#### 4. Conclusions

For the velocity field values obtained in this study, the theoretical semivariogram model that best fits the experimental semivariogram is not necessarily the one that best predicts.

The analysis using the LSC technique shows that the models present values that are very close to the verification values, and better statistics were obtained through cross-validation than in the Kriging method.

With the aforementioned, it was decided to use the method of least squares collocation since it makes a better prediction both for the verification values and for the results obtained in the cross-validation.

#### 6. Referencias citadas

- BANKO, A.; BANKOVIĆ, T.; PAVASOVIĆ, M. & A. ĐAPO. 2020. "An All-in-One Application for Temporal Coordinate Transformation in Geodesy and Geoinformatics". *ISPRS International Journal of Geo-Information*, 9(5): 323.
- BLAIS, J. A. R. 1982 "Synthesis of Kriging estimation methods". *Manuscripta Geodae-tica*, 7(4): 325-352.
- CISNEROS, D. y J. M. NOCQUET. 2011. "Campo de velocidades del Ecuador, obtenido a través de mediciones de campanes GPS de los últimos 15 años y medidas de una red GPS permanente". *Revista Geoespacial*, 9: 30-49.
- CRESSIE, N.A. 1993. *Statistics for Spatial Dat*. John Wiley & Sons. Available from: DOI: 10.1002/9781119115151.
- DA SILVA, L. M.; DE FREITAS, S. R. & R. DALAZOANA. 2018. "Analysis of Dynamic Effects on the Brazilian Vertical Datum". In: YUANZHI ZHANG, YI-JUN HOU & XIAOMEI YANG, IntechOpen Science: *Sea Level Rise and Coastal Infrastructure*. Available from: <http://dx.doi.org/10.5772/intechopen.71546>.
- DARBEHESHTI, N. & W. E. FEATHERSTONE. 2009 "Non-stationary covariance function modelling in 2D least-squares collocation". *Journal of Geodesy*, 83(6): 495-508.
- DENKER, H.; TIMMEN, L.; VOIGT, C.; WEYERS, S.; PEIK, E.; MARGOLIS, H. S.; ... & G. PETIT. 2018. "Geodetic methods to determine the relativistic redshift at the level of  $10^{-18}$  in the context of international timescales: a review and practical results". *Journal of Geodesy*, 92(5): 487-516.

- DERMANIS, A. 1984. "Kriging and collocation: A comparison". *Manuscripta geodaetica*, 9(3): 159-167.
- DERMANIS, A. 1980. "Adjustment of geodetic observations in the presence of signals. Proceedings of the international school of advanced geodesy". *Bollettino di Geodesia e Scienze Affini*, 38: 419-445.
- DOW, J. M.; NEILAN, R. E. & C. RIZOS. 2009. "The international GNSS service in a changing landscape of global navigation satellite systems". *Journal of geodesy*, 83(3): 191-198.
- DREWES, H. & O. O. HEIDBACH. 2005. "Deformation of the South American crust estimated from finite element and collocation methods". In: F. SANSÒ (Ed.), *A Window on the Future of Geodesy, IAG Symposium*, 128: 544-549.
- EROL, S. & B. EROL. 2021. "A comparative assessment of different interpolation algorithms for prediction of GNSS/levelling geoid surface using scattered control data". *Measurement*, 173: 108623.
- FORSBERG, R. 1987. "A new covariance model for inertial gravimetry and gradiometry". *Journal of Geophysical Research: Solid Earth*, 92(B2): 1.305-1.310.
- FU, C.; WANG, P.; ZHAO, L. & X. WANG. 2020. "A distance correlation-based Kriging modeling method for high-dimensional problems". *Knowledge-Based Systems*, 206: 106356.
- GILI, J. A.; COROMINAS, J. & J. RIUS. 2000. "Using Global Positioning System techniques in landslide monitoring". *Engineering geology*, 55(3): 167-192.
- GOOVAERTS, P. 1997. *Geostatistics for natural resources evaluation*. Oxford Univ. Press, New York.
- JIANG, C.; QIU, H.; GAO, L.; WANG, D.; YANG, Z. & L. CHEN. 2020. "Real-time estimation error-guided active learning Kriging method for time-dependent reliability analysis". *Applied Mathematical Modelling*, 77: 82-98.
- JOHNSTON K.; VER HOEF, J. M.; KRIVORUCHKO, K & N. LUCAS. 2001. *Using ArcGIS geostatistical analyst*, vol 380. Esri Redlands.
- JOURNEL, A. G. & C. H. J. HUIJBREGTS. 1991. *Mining Geostatistics*. Academic. New York, USA.
- JOURNEL, A. G. & C. H. J. HUIJBREGTS. 1978. *Mining geostatistics*. Academic Press. New York, USA.
- KEARSLEY, W. 1977. *Non-stationary estimation in gravity prediction problem*. Report 256, Department of Geodetic Science. The Ohio State University, Columbus, USA.
- KESUMA, Z. M.; RAHAYU, L. & A. F. ZOHRA. 2019. Identification of new positive tuberculosis cases in Aceh Besar District using ordinary Criging. *International Conference on Statistics and Analytics (ICSA)* (pp. 29-39).

- KNUDSEN, P. 1987. "Estimation and modelling of the local empirical covariance function using gravity and satellite altimeter data". *Bulletin Geodesique*, 61(2): 145-160.
- KRARUP, T. 1969. "A contribution to the mathematical foundation of physical geodesy". *Geod. Inst. Copenhagen, Medd.*, 44(80): 44.
- LEICK, A. 1995. *GPS Satellite Surveying*. John Willey & Sons, Inc. New York, USA.
- LIGAS, M. & M. KULCZYCKI. 2010. "Simple spatial prediction-least squares prediction, simple kriging, and conditional expectation of normal vector". *Geodesy and Cartography*, 59(2): 69-81.
- LIN, P.; HE, Z.; DU, J.; CHEN, L.; ZHU, X. J. & LI. 2018. "Impacts of climate change on reference evapotranspiration in the Qilian Mountains of China: Historical trends and projected changes". *International Journal of Climatology*, 38(7): 2.980-2.993.
- LING, C.; LU, Z. & K. FENG. 2019. "An efficient method combining adaptive Kriging and fuzzy simulation for estimating failure credibility". *Aerospace Science and Technology*, 92: 620-634.
- LOBO, V. G. & T. C. FONSECA. 2020. "Bayesian residual analysis for spatially correlated data". *Statistical Modelling*, 20(2): 171-194.
- LUNA, M. P.; A. STALLER, A.; T. TOULKERIDIS & H. PARRA. 2017. "Methodological approach for the estimation of a new velocity model for continental Ecuador". *Open Geosciences*, 9(1): 719-734.
- MATHER, R. S.; RIZOS, C.; COLEMAN, R. & E. G. MASTERS. 1979. "Geodetic reference systems for crustal motion studies". *Tectonophysics*, 52(1-4): 15-37.
- MATHERON, G. 1971. *The theory of regionalized variables and its applications*. (Vol. 5). École National Supérieure des Mines, 211. Paris, France.
- MICHAEL, R.; O'LENICK, C. R.; MONAGHAN, A.; WILHELMI, O.; WIEDINMYER, C.; HAYDEN, M. & M. ESTES. 2019. "Application of geostatistical approaches to predict the spatio-temporal distribution of summer ozone in Houston, Texas". *Journal of exposure science & environmental epidemiology*, 29(6): 806-820.
- MONTECINO, H. D.; DE FREITAS, S. R.; BÁEZ, J. C. & V. G. FERREIRA. 2017. "Effects on Chilean Vertical Reference Frame due to the Maule Earthquake co-seismic and post-seismic effects". *Journal of Geodynamics*, 112: 22-30.
- MORITZ, H. 1980. *Advanced physical geodesy*. Herbert Winchmann Verlag, Karlsruhe, Abacus Press. Tunbridge Wells. Kent, Germany.
- MORITZ, H. 1978. "Least-squares collocation". *Rev. Geophys.*, 16(3): 421-430. Available from: <https://doi.org/10.1029/RG016i003p00421>.

- OBROŚLAK, R. & O. DOROZHYNKY. 2017. "Selection of a semivariogram model in the study of spatial distribution of soil moisture". *Journal of Water and Land Development*, 35: 161-166. Available from: <https://doi.org/10.1515/jwld-2017-0080>.
- ODERA, P. A.; Y. FUKUDA & Y. KUROISHI. 2012. "A high-resolution gravimetric geoid model for Japan from EGM2008 and local gravity data". *Earth, planets and space*, 64(5): 361-368.
- OREJUOLA, I. P.; GONZÁLEZ, C. L.; GUERRA, X. B.; MORA, E. C. & T. TOULKERIDIS. 2021. "Geoid undulation modeling through the Cokriging method-A case study of Guayaquil, Ecuador". *Geodesy and Geodynamics*, 12(5): 356-367.
- PASCUALSÁNCHEZ, J. F. 2007. "Introducing relativity in global navigation satellite systems". *Annalen der Physik*, 16(4): 258-273.
- PEREZ, J. A. S.; MONICO, J. F. G. & J. C. CHAVES. 2003. "Velocity field estimation using GPS precise point positioning: the South American plate case". *Journal of Global Positioning Systems*, 2(2): 90-99.
- RAJNER, M. & T. LIWOSZ. 2017. "Analysis of seasonal position variation for selected GNSS sites in Poland using loading modelling and GRACE data". *Geodesy and Geodynamics*, 8(4): 253-259.
- REGUZZONI, M.; F. SANSONO, F. & G. VENUTI. 2005. "The theory of general kriging, with applications to the determination of a local geoid". *Geophys J Int.*, 162: 303-314. Available from: <https://doi.org/10.1111/j.1365-246X.2005.02662.x>.
- RUMMEL, R. 1976. "A model comparison in least squares collocation". *Bulletin géodésique*, 50(2): 181-192.
- SÁNCHEZ, L. & H. DREWES H. 2020. Geodetic monitoring of the variable surface deformation in Latin America. *International Association of Geodesy Symposia Series*, 152.
- SANCHEZ, L.; CIOCE, V.; DREWES, H.; BRUNINI, C.; DE ALMEIDA, M. A.; GAYTAN, G.; ... & S. RUDENKO. 2018. Time evolution of the SIRGAS reference frame. *42nd COSPAR Scientific Assembly*, 42: B2-1.
- SCHAFFRIN, B. 1989. "An alternative approach to robust collocation". *Bulletin géodésique*, 63(4): 395-404.
- SCULL, P.; OKIN, G.; CHADWICK, O. A. & J. FRANKLIN. 2005. "A comparison of methods to predict soil surface texture in an alluvial basin". *The Professional Geographer*, 57(3): 423-437.
- SEVILLA, M. J. 1987. "Colocación mínimos cuadrados", *CSIC-UCM-Instituto de Astronomía y Geodesia (IAG)*. Publicación N° 157, pp. 97-141. Madrid, España.
- SHAPEEV, V.; GOLUSHKO, S.; BRYNDIN, L. & V. BELYAEV. 2019. The least squares collocation method for the biharmonic equation in irregular and mul-

- tiply-connected domains. *Journal of Physics: Conference Series* (Vol. 1.268, No. 1, p. 012076). IOP Publishing.
- SHUKLA, K.; KUMAR, P.; MANN, G. S. & M. KHARE. 2020. "Mapping spatial distribution of particulate matter using Kriging and Inverse Distance Weighting at supersites of megacity Delhi". *Sustainable cities and society*, 54: 101997. Available from: <https://doi.org/10.1016/j.scs.2019.101997>.
- TIERRA, A. 2016. "Prediction 3-D velocity for Ecuador by Artificial Neural Network RBF". *IEEE Latin America Transactions*, 14(1): 386-390.
- TSCHERNING, C. C. 1976. *Covariance expressions for second and lower order derivatives of the anomalous potential*. Department of Geodetic Science, Ohio State University.
- VERMA, R. R.; MANJUNATH, B. L.; SINGH, N. P.; KUMAR, A.; ASOLKAR, T.; CHAVAN, V., ... & P. SINGH. 2018. "Soil mapping and delineation of management zones in the Western Ghats of coastal India". *Land Degradation & Development*, 29(12): 4.313-4.322.
- WEBSTER, R. & M. A. OLIVER. 2007. *Geostatistics for environmental scientists*. John Wiley & Sons.
- WILDE, F.; GAMMEL, B. M. & M. PEHL. 2018. "Spatial correlation analysis on physical unclonable functions". *IEEE Transactions on Information Forensics and Security*, 13(6): 1.468-1.480.
- XIAO, S.; OLADYSHKIN, S. & W. NOWAK. 2020. "Reliability analysis with stratified importance sampling based on adaptive Kriging". *Reliability Engineering & System Safety*, 197: 106852.
- XIE, Y.; EFTELIOGLU, E.; ALI, R. Y.; TANG, X.; LI, Y.; DOSHI, R. & S. SHEKHAR. 2017. "Transdisciplinary foundations of geospatial data science". *ISPRS International Journal of Geo-Information*, 6(12): 395.
- YAN, X.; FENG, Y.; TONG, X.; LI, P.; ZHOU, Y.; WU, P.; ... & WANG, C. 2021. "Reducing spatial autocorrelation in the dynamic simulation of urban growth using eigenvector spatial filtering". *International Journal of Applied Earth Observation and Geoinformation*, 102: 102434.
- YANG, X. & X. CHENG. 2020. "Active learning method combining Kriging model and multimodal-optimization-based importance sampling for the estimation of small failure probability". *International Journal for Numerical Methods in Engineering*, 121(21): 4.843-4.864.
- YANG, Y. & X. QIN. 2021. "Resilient observation models for seafloor geodetic positioning". *Journal of Geodesy*, 95(7): 1-13.
- ZENG, F.; TURNER, I.; BURRAGE, K. & S. J. WRIGHT. 2019. "A discrete least squares collocation method for two-dimensional nonlinear time-dependent partial differential equations". *Journal of Computational Physics*, 394: 177-199.